

# Influence of Polymer Viscoelasticity on the Residence Distributions of Extruders

**Paul Elkouss and David I. Bigio**

Dept. of Mechanical Engineering, University of Maryland, College Park, MD 20742

**Mark D. Wetzel**

E.I. du Pont de Nemours & Co., Experimental Station, Wilmington, DE 19880

**Srinivasa R. Raghavan**

Dept. of Chemical Engineering, University of Maryland, College Park, MD 20742

DOI 10.1002/aic.10754

Published online January 6, 2006 in Wiley InterScience (www.interscience.wiley.com).

*Fluid flow in extruders has been described kinematically using residence time distributions (RTDs). Residence Distributions (RxD), as expressed by Residence Volume Distributions and Residence Revolution Distributions, have shown to collapse the RTD curves onto single master curves based on specific throughput. When the same extruder is used for processing different polymers, differences in RxDs have been attributed mainly to differences in material viscosity, as measured, for example, by the melt flow index. This study explores the role of polymer viscoelasticity in modeling extruder performance. It is shown that viscosity is not the material property that explains differences in RxDs. In one case, two materials with very similar viscosities have very different RxDs and, in a second case, two materials having very different viscosities have very similar RxDs. A calculation of the Weissenberg number for each system shows that viscoelastic effects can underlie the differences in RxD. Strongly elastic fluids tend to travel in a plug-flow-like manner down an extruder and so their RxDs are qualitatively different from those of viscous fluids. The results thus show that comprehensive rheological information is necessary for modeling the flow of polymer melts in extruders. © 2006 American Institute of Chemical Engineers AIChE J, 52: 1451–1459, 2006*

*Keywords: twin-screw extruder, residence distributions, rheology, elasticity, polypropylene, polyethylene*

## Introduction

Extruders are used to continuously process polymeric materials. The interplay between extruder configuration, operating conditions, and polymer rheology is important in dictating the final properties of the extrudate. The rheological properties of the polymer have a significant impact on fluid flow in an

extruder. Selection of polymer grades is often done by examining manufacturer-supplied melt flow index (MFI) values. However, when suppliers change formulations of polymers, rheological properties can be different in spite of consistent MFI values. This study explores the influence of rheological properties on polymer extrusion.

An extruder is composed of a barrel that houses screws or shafts that convey and mix material over the length of the machine. An intermeshing, corotating twin-screw extruder (CoTSE) has two screws composed of different elements that are self-wiping and rotate in the same direction. The machine

Correspondence concerning this article should be addressed to D. I. Bigio at bigio@eng.umd.edu.

can be designed to process the material in a variety of ways. Process variables include the barrel and feeding arrangement, the screw geometry, and operating conditions such as volumetric throughput  $Q$ , screw speed  $N$ , and barrel temperatures.

Determination of optimal process design is not trivial for extrusion operations. The CoTSE has a complicated geometry that makes it difficult to compute fluid dynamics of the entire machine. Comparisons of different extruder geometries and different feed materials have typically been performed using the residence time distribution (RTD). The RTD measures how long material takes to pass a given point and is used as a kinematic description of the flow, to understand the axial mixing in the machine. Various combinations of mixing elements in the CoTSE have been studied to show their effect on mean residence time and RTD.

When residence time distributions are presented in the time domain, any change of screw speed or volumetric throughput results in a different curve. RTDs, however, can be normalized by screw speed or volumetric throughput, to create residence rotation distributions (RRDs) and residence volume distributions (RVDs). In a recent study, Bigio et al.<sup>1</sup> showed, rather surprisingly, that for the same *specific* throughput ( $Q/N$ , the ratio of volumetric throughput to screw speed), the RRD plots superpose. Additionally, when the same data were plotted as RTDs without the transport delay, the curves again superposed onto a mastercurve. Thus, the RRD and RVD were shown to be independent of the extrusion conditions (screw speeds, shear rates) and were essentially characteristic of the material. It should be noted that the polymer used here was a high-density polyethylene (HDPE), a polymer with non-Newtonian rheology.

In addition to geometry and operating conditions, the rheology of the polymer plays a critical role in dictating the process response as well as the ultimate properties of the extrudate. A simplistic view of the extrusion process would predict (erroneously) that materials with *similar viscosities* would exhibit *similar RTDs*. Herein, we demonstrate that this is not necessarily the case. Our extrusion studies show that even when polymers have very different viscosities, the RTDs for the extrusion can be very similar. On the other hand, polymers with similar viscosities can exhibit very different RTDs during extrusion.

## Background

### *Residence distributions for polymer extrusion*

RTDs for polymer extrusion in the CoTSE have been studied by several researchers. The influence of polymer rheology on extrusion was investigated by Dealy et al.,<sup>2</sup> who showed that the mean residence time increased with decreasing polymer viscosity and with higher screw speeds. Hu et al.<sup>3,4</sup> developed a model for the RTD in an extruder, with the assumption that perfect mixing exists at the boundary of divided screw elements. Bigio et al.<sup>1</sup> presented a predictive RTD model (Eq. 1), where  $a$  is a shape factor and  $t_d$  is the delay time. This equation models the extruder as being composed of three filled regions and three partially filled regions, with the latter acting as transport delays before each filled region. The filled regions in this context are the melting, mixing, and die zones.

$$G(t) = \frac{a^3}{2} e^{-a(t-t_d)} \quad (1)$$

This equation was developed for an extruder with a single probe at the outlet measuring the RTD response. The same shape factor can thus be used for each zone. Bigio et al.<sup>1</sup> also expressed the model in the Laplace domain as follows:

$$G(s) = \frac{a^3 e^{-st_d}}{(s+a)^3} \quad (2)$$

Here, the shape factor  $a$  is the inverse of the characteristic time for each filled region of the extruder. The shape of the RTD is dominated by throughput for a screw configuration and material combination. Constant  $N$  and increasing  $Q$  move the RTD to shorter times and make it sharper. Constant  $Q$  and increasing  $N$  move the RTD to shorter times, while changing the shape minimally.

Residence distributions have also been studied in two other domains. The RRD is made by normalizing the time axis by the number of accumulated screw revolutions ( $t \times N$ ). The RVD is made by plotting the tracer concentration over an accumulated volume ( $t \times Q$ ) of extrudate. Bigio et al.<sup>1</sup> showed that for the extrusion of the same material at different operating conditions, the RVD and RRD curves superposed if they were compared at the same  $Q/N$ . This has the following meaning. Suppose for a given specific throughput  $Q/N$ , the first trace in the RVD curve appeared after 10 “volumes,” the maximum occurred at 15 “volumes,” and the trace was gone by 20 “volumes.” Then if the operating conditions were changed, but the specific throughput  $Q/N$  was held constant, the delay time and the shape of the RVD curve would be exactly the same. Thus, even at the new operating conditions, the first trace would appear at 10 “volumes,” the maximum at 15 “volumes,” and the trace would end by 20 “volumes.” The authors cautioned that “this result needs to be interpreted against the fact that the rheology changes with screw speed.” We explore this statement in this article.

The RVD mastercurve indicates that residence distributions have very similar shape factors in the volume domain, which shows that the axial distribution of the tracer is not dependent on the operating conditions for a given screw geometry. The same volume domain shape factor can be used to describe a family of curves for various operating conditions. Additionally larger  $Q/N$  leads to a larger delay volume ( $v_d$ ) and smaller screw-revolution delay ( $n_d$ ).

### *Polymer rheology and shear flow*

The flow of polymeric fluids can be characterized using the Weissenberg number ( $Wi$ ). For a shear flow, this dimensionless quantity is the product of the longest relaxation time of the polymer ( $\lambda$ ) and the characteristic shear rate ( $\dot{\gamma}$ ), that is,  $Wi = \lambda \dot{\gamma}$ . At low shear rates ( $\dot{\gamma} < 1/\lambda$ ), that is, for  $Wi < 1$ , the polymer coil is able to relax within the timescale of the flow. On the other hand, at high shear rates ( $\dot{\gamma} > 1/\lambda$ ), that is, for  $Wi > 1$ , the polymer coil becomes progressively stretched and is unable to relax to its coil-like state. Thus polymer molecules show qualitatively different behavior at low and high Weissenberg numbers. The longest relaxation time  $\lambda$  of the polymer can

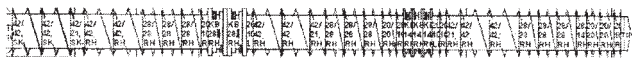


**Figure 1. Experimental screw design.**

be obtained from a dynamic rheological experiment as the inverse of the frequency at which the storage modulus  $G'$  and loss modulus  $G''$  cross.

A calculation of the Weissenberg number can be instructive in terms of the interplay between fluid rheology and process conditions. In the case of a viscous, Newtonian fluid, the relaxation time is very low and therefore  $Wi$  remains  $<1$  for most practical shear rates. On the other hand, viscoelastic polymeric fluids have a finite relaxation time. In the latter case, the  $Wi$  can exceed 1 at practical shear rates, which leads to a behavior dominated by the elasticity of the polymer molecules. Note that in the high  $Wi$  regime, the sample will be shear-thinning, that is, the viscosity will be a decreasing function of shear rate. Under these conditions, the flow in the extruder will become pluglike, in contrast to the parabolic velocity profile exhibited by Newtonian materials.

## Experimental

### Extruder design

A ZSK-30 CoTSE (Coperion-Werner & Pfeleiderer GmbH, Stuttgart, Germany) with a 30-mm screw diameter was used in this study. The extruder screw is designed to create three regions of complete melt fill, referred to as the melting, mixing, and die zones. These zones are created by a pressure obstruction being placed on the screw. In the first two zones, a reverse-thread screw element is used; in the third zone, the die-hole pressure causes fluid buildup. The screw configuration is shown in Figure 1.

### Polymers and extrusion conditions

Two polypropylenes (PPs; Montell KF6100 and Basell PDC1277, Basell Polyolefins B.V., Hoofddorp, The Netherlands) and two polyethylenes (PEs; Alathon<sup>®</sup> HDPE 6018 and Alathon<sup>®</sup> HDPE 6060, Equistar Chemical Co., San Antonio, TX) were used. The two polypropylenes (which will be denoted as PP 6100 and PP 1277 henceforth) have the same MFI of 3 g/10 min, whereas the MFIs of the HDPE 6018 and the HDPE 6060 are 18 and 6 g/10 min, respectively (all values reported by the respective manufacturers). The polypropylenes were extruded at 210°C, whereas the polyethylenes were processed at 180°C.

### RTD measurement

RTDs for the extrusion process were determined by a reflectance method, as described by Wetzel et al.<sup>5</sup> Reflectance probes were placed past the tips of the screws just before the die and mixing zones. Premixed pellets containing  $TiO_2$  were added to the feed and the response can be considered an impulse response. The data were collected at a sampling rate of 60 Hz, which is well above the screw speed, and then down-sampled to 20 Hz. Three replicates of each run were conducted and the data were averaged, filtered, and normalized.

### Rheology measurements

The melt rheology of the four polymers was examined using a Rheometrics RDA-III rheometer (TA Instruments, New Castle, DE) at their respective processing temperatures. Samples were examined in oscillatory shear and both the viscoelastic moduli and the complex viscosity were measured as a function of the frequency of oscillations. The strain amplitude was held constant at 5% during this experiment, which falls well within the linear viscoelastic regime

**Table 1. Experimental Results for Polyethylene RTD Experiments**

Polymer	#	$Q$ (mL/s)	$N$ (rps)	$Q/N$ (mL/r)	$N/Q$ (r/mL)	$a$ (1/s)	$c$ (1/mL)	$t_d$ (s)	$t_m$ (s)
HDPE 6018	1	1.67	1.75	0.95	1.05	0.0904	0.0542	52.3	85.4
	2	1.67	3.50	0.48	2.10	0.0859	0.0515	39.8	74.7
	3	3.33	2.33	1.43	0.70	0.2028	0.0608	36.4	51.2
	4	3.33	3.50	0.95	1.05	0.2144	0.0643	28.9	42.9
	5	3.33	4.42	0.75	1.33	0.2056	0.0617	25.3	39.9
	6	3.33	5.83	0.57	1.75	0.1858	0.0557	19.2	35.3
	7	5.00	2.67	1.87	0.53	0.2844	0.0569	27.9	38.4
	8	5.00	3.50	1.43	0.70	0.2906	0.0581	22.9	33.3
	9	5.00	5.33	0.94	1.07	0.2808	0.0562	17.8	28.5
	10	6.67	2.83	2.35	0.42	0.3532	0.0530	22.7	31.2
	11	6.67	3.50	1.90	0.52	0.3175	0.0476	19.3	28.7
	12	6.67	4.67	1.43	0.70	0.3737	0.0561	17.0	25.0
HDPE 6060	1	1.67	1.75	0.95	1.05	0.0868	0.0521	51.6	86.1
	2	1.67	3.50	0.48	2.10	0.0821	0.0493	35.9	72.4
	3	3.33	2.33	1.43	0.70	0.1787	0.0536	31.5	48.3
	4	3.33	3.50	0.95	1.05	0.1832	0.0550	24.8	41.2
	5	3.33	4.42	0.75	1.33	0.1894	0.0568	22.2	38.1
	6	3.33	5.83	0.57	1.75	0.1878	0.0563	19.6	35.6
	7	5.00	2.67	1.87	0.53	0.2631	0.0526	25.0	36.4
	8	5.00	3.50	1.43	0.70	0.2735	0.0547	20.3	31.3
	9	5.00	5.33	0.94	1.07	0.2775	0.0555	15.7	26.5
	10	6.67	2.83	2.35	0.42	0.3517	0.0528	21.2	29.7
	11	6.67	3.50	1.90	0.52	0.3612	0.0542	18.5	26.8
	12	6.67	4.67	1.43	0.70	0.3456	0.0518	14.9	23.6

**Table 2. Experimental Results for Polypropylene RTD Experiments**

Polymer	#	$Q$ (mL/s)	$N$ (rps)	$Q/N$ (mL/r)	$N/Q$ (r/mL)	$a$ (1/s)	$c$ (1/mL)	$t_d$ (s)	$t_m$ (s)
PP 6100	1	1.49	1.75	0.85	1.17	0.1359	0.0912	45.4	67.5
	2	1.49	3.50	0.43	2.35	0.1442	0.0968	30.4	51.3
	3	2.98	2.33	1.28	0.78	0.2077	0.0697	33.4	47.9
	4	2.98	3.50	0.85	1.17	0.2230	0.0748	25.5	39.0
	13	2.98	3.50	0.85	1.17	0.2885	0.0968	23.5	33.9
	5	2.98	4.42	0.67	1.48	0.1995	0.0669	20.0	35.1
	6	2.98	5.83	0.51	1.96	0.4289	0.1439	19.8	26.8
	7	4.47	2.67	1.68	0.60	0.3657	0.0818	24.4	32.6
	8	4.47	3.50	1.28	0.78	0.4513	0.1009	20.1	26.7
	14	4.47	3.50	1.28	0.78	0.2883	0.0645	20.3	30.8
	9	4.47	5.33	0.84	1.19	0.4694	0.1050	15.5	21.9
	10	5.96	2.33	2.55	0.39	0.3053	0.0512	26.4	36.2
11	5.96	3.50	1.70	0.59	0.5145	0.0863	19.7	25.5	
12	5.96	4.67	1.28	0.78	0.7268	0.1219	15.6	19.8	
PP 1277	1	1.49	1.75	0.85	1.17	0.0327	0.0219	66.4	156.5
	2	1.49	3.50	0.43	2.35	0.032	0.0215	46.9	139.3
	3	2.98	2.33	1.28	0.78	0.0644	0.0216	42.3	88.7
	4	2.98	3.50	0.85	1.17	0.0586	0.0197	31.9	82.8
	5	2.98	4.42	0.67	1.48	0.0565	0.0190	24.1	76.9
	6	2.98	5.83	0.51	1.96	0.0579	0.0194	22.2	73.8
	7	4.47	2.67	1.68	0.60	0.092	0.0206	33.5	66.1
	8	4.47	3.50	1.28	0.78	0.0885	0.0198	27.1	61.0
	9	4.47	5.33	0.84	1.19	0.0934	0.0209	21.0	53.2
	10	5.96	2.67	2.24	0.45	0.1045	0.0175	28.9	57.6
	11	5.96	3.50	1.70	0.59	0.1176	0.0197	25.1	50.6
	12	5.96	4.67	1.28	0.78	0.1129	0.0189	19.2	45.8

of the polymers studied. For linear polymers, the Cox–Merz rule is expected to hold, so that the complex viscosity as a function of frequency can be equated to the steady viscosity vs. shear rate.

**Results and Discussion**

**Residence distributions**

Each of the four polymers was processed in the CoTSE at the same operating conditions, as presented in Tables 1 and 2. These conditions were chosen to represent the range of normal extruder operation and to create a broad range of specific throughputs  $Q/N$ , some of which are repeated at different values of volumetric flow rate  $Q$  and screw speed  $N$ . Figure 2 shows the normalized RTD for the HDPE 6018 and the corresponding normalized RVD is shown in Figure 3. The RVD plot was constructed by scaling the RTD data with volumetric flow rate  $Q$  and removing the delay times. Consistent with our earlier observations, we find that the RVDs for this HDPE under various operating conditions overlap to form a mastercurve. Note that both the mean and the amplitudes for the various individual RVD curves are practically identical. It should be pointed out that, over the operating range tested, the polymer underwent a more than threefold increase in average shear rate, which in turn must have caused a commensurate decrease in viscosity. Despite these rheological changes, the RVD curves have the same shape.

Similar plots of RTD (Figure 4) and RVD (Figure 5) are shown for the HDPE 6060. Here again, the RVD plots overlap to form a mastercurve once the delay times are removed and, again, the mean and the curve shapes are identical within experimental accuracy. As before, the curves overlap for operating conditions corresponding to a range of shear rates and polymer viscosities, which are dependent on shear rate. A

further significant observation is that the RVDs for the two HDPEs are themselves identical to each other—in other words, Figures 3 and 5 overlay almost perfectly. This means that, for two different HDPEs with MFIs differing by a factor of 6, the RVD plots are essentially the same. These results highlight the insignificance of viscosity in dictating extruder RTD over the operating range tested.

Next, a similar analysis is performed for the two polypropylenes under investigation. Figure 6 shows the RTD for the PP 1277 and Figure 7 shows the corresponding normalized RVD. Just as for the two HDPE polymers, the RVD for this PP essentially follows a mastercurve once the delay times are

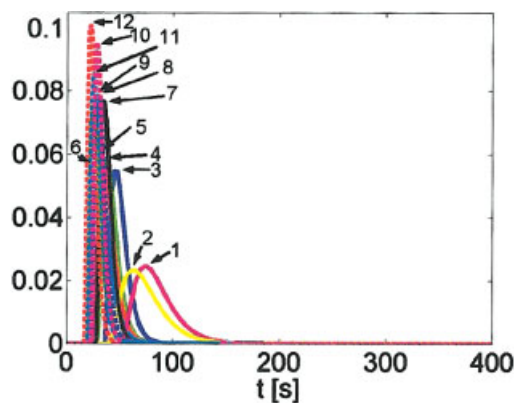


**Figure 2. Normalized residence time distributions for the HDPE 6018 at various operating conditions.**

The numbers pointing to each curve correspond to those in the # column of Table 1. [Color figure can be viewed in the online issue, which is available at [www.interscience.wiley.com](http://www.interscience.wiley.com).]

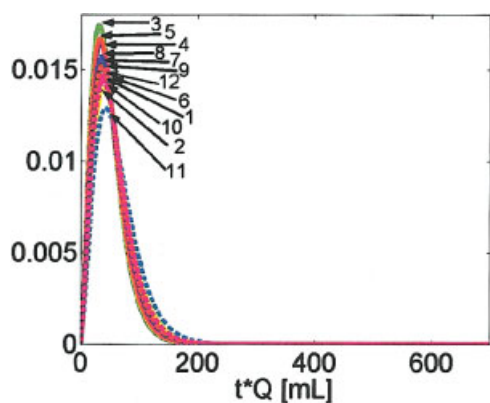


**Figure 3. Normalized residence volume distributions for the HDPE 6018 at various operating conditions.**

The numbers pointing to each curve correspond to those in the # column of Table 1. [Color figure can be viewed in the online issue, which is available at [www.interscience.wiley.com](http://www.interscience.wiley.com).]

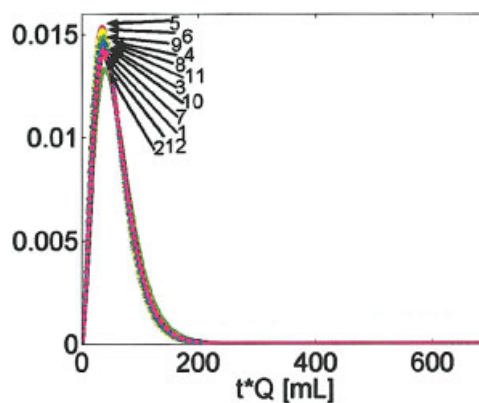


**Figure 5. Normalized residence volume distributions for the HDPE 6060 at various operating conditions.**

The numbers pointing to each curve correspond to those in the # column of Table 1. [Color figure can be viewed in the online issue, which is available at [www.interscience.wiley.com](http://www.interscience.wiley.com).]

removed. In this case, there is slightly more variation to the shape of the plot and the mean volume varies slightly. Thus, the scatter of the data is larger for this polymer than that for the two HDPEs. Finally, Figure 8 shows the RTD for the polypropylene PP 6100 and Figure 9 shows the corresponding RVD. In this case, the RVD plots clearly *do not* overlap onto a single curve. Individual curves are observed to have different shapes and the mean “volume” changes in a nonobvious fashion. Thus, the PP 6100 shows a very different behavior in the extruder compared to that of the other three polymers studied.

To further understand these results, we use the model proposed by Bigio et al. to describe the residence distributions and we then compare the model results. The key parameter in describing each distribution (RTD or RVD) is the shape factor. Similar shape factors indicate similar shapes of the curves. A smaller shape factor indicates more spread in the distribution, or a wider curve. For RVDs, Bigio et al. derive the following equation using the conversions in Eq. 4. It was found that one

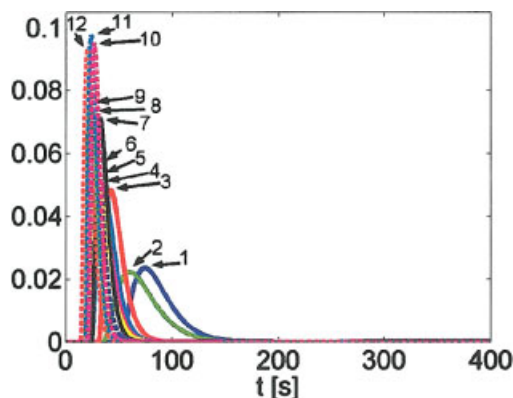
value of the volume domain shape factor  $c$  can represent a family of curves:

$$\hat{G}(\hat{s}) = \frac{c^3 e^{-\hat{s}c}}{(\hat{s} + c)^3} \quad (3)$$

$$a = cQ \quad s = \hat{s}Q \quad (4)$$

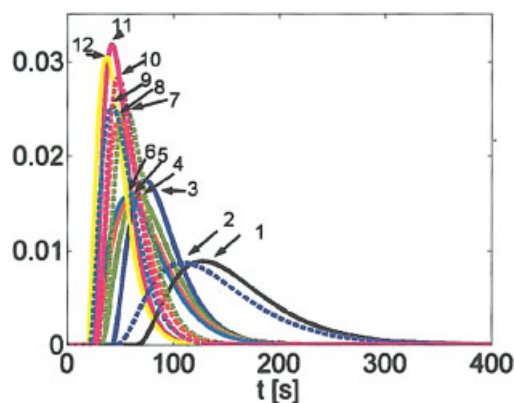
Tables 1 and 2 show the shape factors for each curve and Table 3 shows the means of the volume domain shape factors. Figure 10 plots the volume-domain shape factor vs. the screw speed for the two HDPEs. The volume-domain shape factor  $c$  is observed to be independent of screw speed for each of the HDPEs and, moreover, its value for both polymers is also identical. The constant value of this shape factor again illustrates how similar their RTDs are and that the extruder response is not a function of viscosity.

Figure 11 plots the volume-domain shape factor for the two polypropylenes, PP 1277 and PP 6100. The shape factor for the



**Figure 4. Normalized residence time distributions for the HDPE 6060 at various operating conditions.**

The numbers pointing to each curve correspond to those in the # column of Table 1. [Color figure can be viewed in the online issue, which is available at [www.interscience.wiley.com](http://www.interscience.wiley.com).]



**Figure 6. Normalized residence time distributions for the PP 1277 at various operating conditions.**

The numbers pointing to each curve correspond to those in the # column of Table 2. [Color figure can be viewed in the online issue, which is available at [www.interscience.wiley.com](http://www.interscience.wiley.com).]

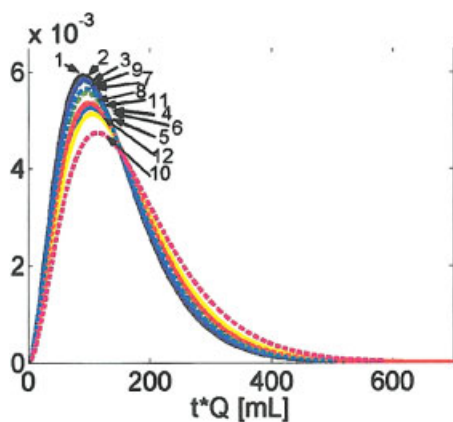


**Figure 7. Normalized residence volume distributions for the PP 1277 at various operating conditions.**

The numbers pointing to each curve correspond to those in the # column of Table 2. [Color figure can be viewed in the online issue, which is available at [www.interscience.wiley.com](http://www.interscience.wiley.com).]

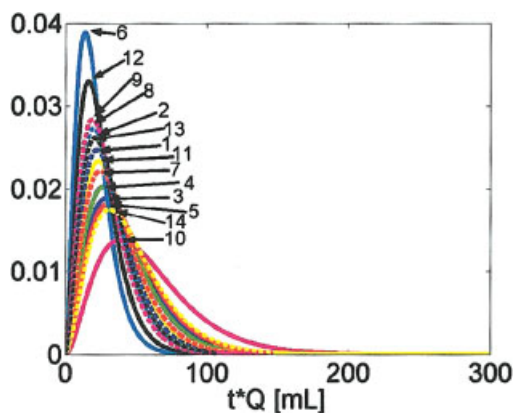


**Figure 9. Normalized residence volume distributions for the PP 6100 at various operating conditions.**

The numbers pointing to each curve correspond to those in the # column of Table 2. [Color figure can be viewed in the online issue, which is available at [www.interscience.wiley.com](http://www.interscience.wiley.com).]

PP 1277 is constant and half the corresponding value obtained for the two HDPEs. The constancy of the shape factor confirms the validity of an RVD mastercurve, as observed in Figure 6. Finally, Figure 11 shows that the volume-domain shape factor for the PP 6100 is not constant. Indeed, Table 3 shows that the standard deviation for the PP 6100 shape factor was an order of magnitude higher than that of the other materials. It could be argued from Figure 11 that the shape factor is essentially constant for screw speeds < 3 rps. For screw speeds above that value, the shape factor increases, which means that the RVD becomes less spread, that is, axial mixing is lower.

### Polymer rheology

Rheological tests were conducted on the polymers to probe the underlying causes for the RVD results. Figure 12 shows the storage modulus  $G'$  and the loss modulus  $G''$  as functions of frequency for the two HDPEs at 180°C (that is, the temperature at which the polymers were extruded). For both polymers,  $G''$  exceeds  $G'$  over the entire range of frequencies studied. It is

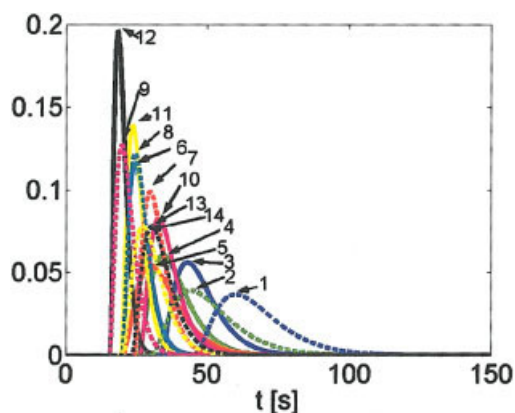


**Figure 8. Normalized residence time distributions for the PP 6100 at various operating conditions.**

The numbers pointing to each curve correspond to those in the # column of Table 2. [Color figure can be viewed in the online issue, which is available at [www.interscience.wiley.com](http://www.interscience.wiley.com).]

only at high frequencies that the two moduli become comparable, which indicates that the HDPEs behave in a predominantly viscous fashion over the entire range of experimental timescales. In terms of differences between the two HDPEs, the moduli for the HDPE 6060 are about twice those of the HDPE 6018, which suggests that the HDPE 6060 has a higher viscosity (see Figure 15 below for further confirmation).

Figures 13 and 14 show the corresponding  $G'$  and  $G''$  vs. frequency plots for the two PPs at 210°C, which is the temperature at which these polymers were extruded. For clarity, the data have been split into two plots, with Figure 13 showing the response of the PP 1277 and Figure 14 that of the PP 6100. Both polymers show a viscoelastic response in their dynamic rheological spectra. In each case, the response is predominantly elastic at high frequencies (where  $G'$  exceeds  $G''$ ) and viscous at low frequencies (where  $G''$  exceeds  $G'$ ). The cross over from elastic to viscous response occurs at the frequency where  $G'$  and  $G''$  intersect. The inverse of this crossover frequency is the longest relaxation time  $\lambda$  of the polymer, values of which are listed in Table 4 for each polymer. The key difference between the PP 1277 and the PP 6100 is that the relaxation time for the latter is twice as high as that of the former. Indeed, the PP 6100 had by far the highest relaxation time among the four polymers studied. As we will see, this high relaxation time is implicated in the anomalous RTD results observed with this polymer.

The complex viscosity  $\eta^*$  can also be calculated from  $G'$  and  $G''$ . According to the well-known Cox–Merz rule, a plot of complex viscosity vs. frequency is approximately identical to a plot of steady-shear viscosity vs. shear rate. Figure 15 shows that the complex viscosity is lowest for the HDPE 6018, followed by the HDPE 6060. Moreover, the viscosity curves for these two polymers show a plateau at low frequencies and

**Table 3. Mean Shape Factors (in the Volume Domain) for Each Polymer**

Polymer	PP 6100	PP 1277	HDPE 6018	HDPE 6060
Mean $c$ ( $\text{mL}^{-1}$ )	0.0894	0.0200	0.0564	0.0538
Standard deviation $c$	0.0244	0.0013	0.0046	0.0022
% SD $C$	27.30	6.50	8.14	4.14

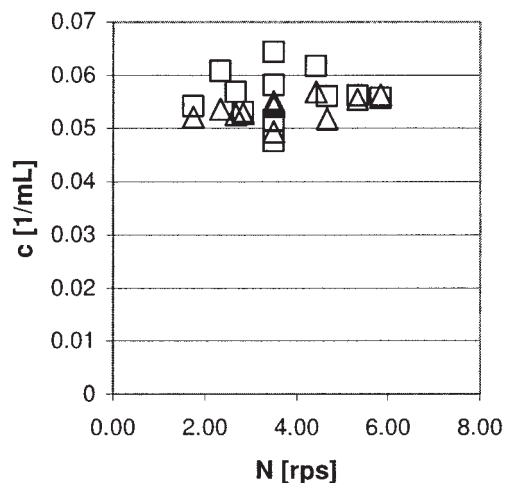


**Figure 10. Volume domain shape factors as a function of screw speed for the two HDPEs.**

The squares and triangles represent HDPE 6018 and HDPE 6060, respectively.

only a slight drop at higher frequencies, which suggests that their behavior is close to Newtonian. With respect to the two PPs, their viscosity curves have a very different shape, lacking a true plateau at low frequencies. Moreover, the viscosity drops sharply and steadily with increasing frequency (shear-thinning behavior). The two PPs have very similar viscosities over the range of frequencies, with the PP 6100 having a slightly higher viscosity in the low-frequency limit.

### Weissenberg number analysis

Based on viscosity alone (Figure 15), one would conclude that the two PPs are quite similar, whereas the HDPEs are very different. As we saw earlier, however, the RVDs for the two PPs are very different, whereas those for the HDPEs are practically identical. To explain these differences further, we must consider the timescales involved in the extruder opera-

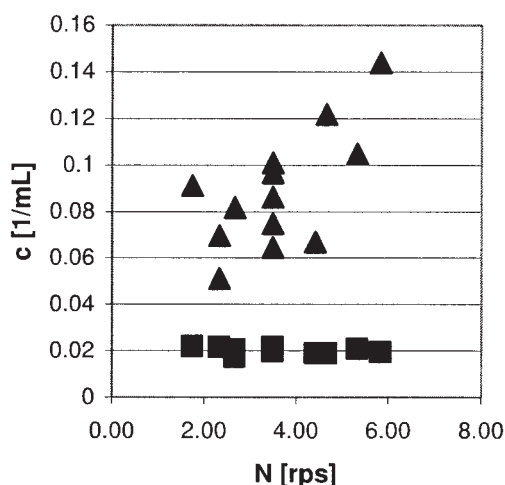


**Figure 11. Volume domain shape factors as a function of screw speed for the two PPs.**

The solid triangles and solid squares represent PP 6100 and PP 1277, respectively.

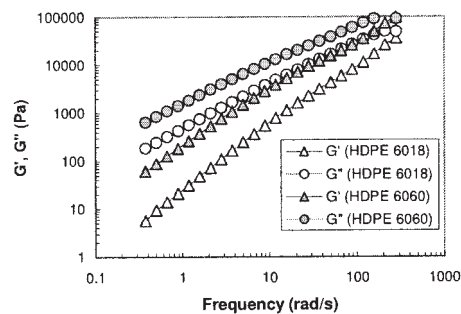


**Figure 12. Storage modulus  $G'$  and loss modulus  $G''$  as functions of frequency for the two HDPEs studied.**

The data were collected at 180°C.

tion. In this context, it is useful to calculate the Weissenberg number ( $Wi$ ) for each polymer for conditions under which it was extruded.  $Wi$  is defined as the product of the relaxation time  $\lambda$  of the polymer and the shear rate  $\dot{\gamma}$  in the extruder. Relaxation times  $\lambda$  of the four polymers obtained from the rheological experiments are shown in Table 4. The shear rate in the extruder is defined as

$$\dot{\gamma} = \frac{\pi DN}{h} \quad (5)$$

where  $D$  is the screw diameter ( $=30$  mm),  $h$  is the channel depth ( $=4.7$  mm), and  $N$  is the screw speed. Thus, the expression for  $Wi$  reduces to

$$Wi = \lambda \dot{\gamma} = \left( \lambda \frac{\pi D}{h} \right) N \quad (6)$$

A plot of  $Wi$  vs. screw speed  $N$  is shown in Figure 16 for the four polymers studied. The two HDPEs both show values of  $Wi \ll 1$  over the entire range of screw speeds. This is to be expected because the relaxation times of both these polymers are very low (Table 4). The PP1277, on the other hand, has a higher relaxation time, and accordingly shows higher  $Wi$  values. Note that the  $Wi$  exceeds 1 at higher values of  $N$ , which

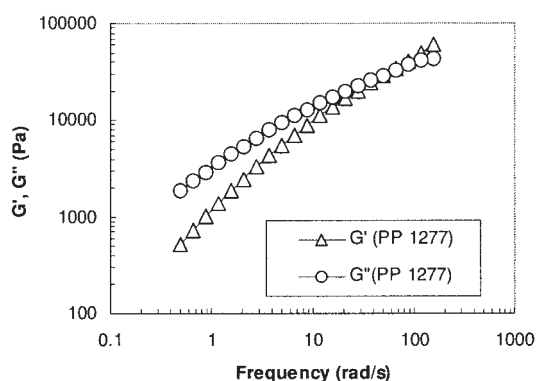


**Figure 13. Storage modulus  $G'$  and loss modulus  $G''$  as functions of frequency for PP 1277.**

The data were collected at 210°C.

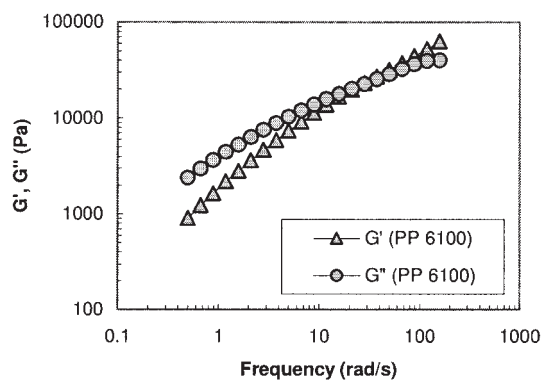


**Figure 14. Storage modulus  $G'$  and loss modulus  $G''$  as functions of frequency for PP 6100.**

The data were collected at 210°C.

means that at a certain screw speed, there is a crossover from a viscous to an elastic regime for this polymer. Finally, the PP6100, which has the highest relaxation time, shows the highest values of  $Wi$ . In this case,  $Wi$  exceeds 1 over the entire range of screw speeds investigated, which means that the behavior of the PP6100 falls in an elastic regime, where the timescale of the flow is faster than the timescale of polymer relaxation. Thus, polymer coils will remain stretched during the flow and will not have sufficient time to unstretch and relax.

The differences in the Weissenberg numbers provide clues to explain the RVD results. Thus, the HDPEs were both extruded at low  $Wi$  ( $\ll 1$ ) and in these cases the RVDs characteristically collapsed to a mastercurve. On the other hand, the PP6100 was studied at high  $Wi$  ( $\gg 1$ ) and in these cases the RVDs did not collapse onto a single curve. The  $Wi$  numbers show that the polymer behaved in an elastic manner under flow. Recall, also, that for the PP6100, as the screw speed increased, the volume-domain shape factor also increased. This increase in shape factor means that there is less axial mixing and that the fluid flow more nearly resembles plug flow. Thus, it is quite plausible that the collapse of RVD curves does not work for highly elastic extrusion flows, where the flow becomes pluglike.

Based on the above analysis, it is clear that the viscoelastic nature of the polymer must be taken into account in analyzing extrusion flows. The characteristic relaxation time  $\lambda$  of the polymer is the key quantity. When  $\lambda$  is large, the elastic effects of the polymer may dominate under typical flow conditions. On the other hand, when  $\lambda$  is low, the flow will be dominated by viscous effects. Indeed, the latter is the case for the two HDPEs. Although the viscosities of the HDPEs were different, in each case the  $\lambda$  was sufficiently low such that  $Wi$  was  $\ll 1$ . Consequently, the HDPEs exhibited RTDs that were very similar for the same operating conditions. Stated differently, we

**Table 4. Weissenberg Number Calculations**

Polymer	Crossover Frequency ( $s^{-1}$ )	Dominant Relaxation Time, $\lambda$ (s)	$\dot{\gamma}$ ( $s^{-1}$ )	$N_{wi}$
PP 1277	58.10	1.72E-02	46.3	0.80
PP 6100	24.63	4.06E-02	46.3	1.88
HDPE 6018	350.67	2.85E-03	46.3	0.13
HDPE 6060	270.50	3.70E-03	46.3	0.17

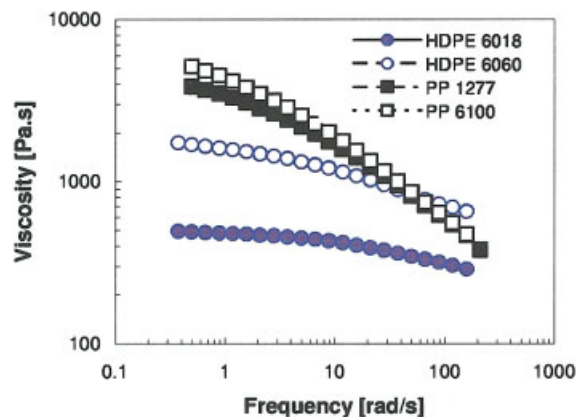


**Figure 15. Complex viscosity as a function of frequency for the four polymers studied.**

The data were calculated using the moduli values in Figures 7 and 8. [Color figure can be viewed in the online issue, which is available at [www.interscience.wiley.com](http://www.interscience.wiley.com).]

can conclude that viscosity is inconsequential with respect to the RVD model, as long as the flow in the extruder is predominantly viscous.

## Conclusion

Operating conditions, machine geometry, and material properties are all important to characterization of extrusion processes. The common understanding that changes in simple measures of viscosity, such as melt flow index or simple shear-dependent viscosity, will directly relate to changes in the residence time distribution is not necessarily true. In contrast to this idea, experiments have shown that the residence distribution (RxD) approach—residence volume distribution (RVD) and residence rotation distribution (RRD)—is a powerful model for normalizing and characterizing extruder performance. For the same extrusion process, two polyethylenes, with very different viscosities, had very similar RVDs and two polypropylenes, with very similar viscosities, had very differ-

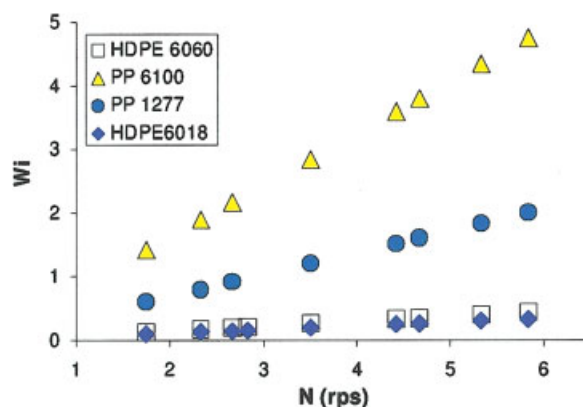


**Figure 16. Weissenberg number ( $Wi$ ) as a function of screw speed for the four polymers tested.**

The PP 6100 shows values of  $Wi > 1$  over the entire range of  $N$ . [Color figure can be viewed in the online issue, which is available at [www.interscience.wiley.com](http://www.interscience.wiley.com).]

ent RVDs. Also, both of the HDPEs and one of the PPs followed the RVD model as previously published.

Rheological tests were conducted on the polymers to probe the underlying causes for the RVD results. When the materials behave in a predominantly viscous fashion over the entire range of experimental timescales, as was the case for both of the HDPEs and one of the PPs, the RVD model proves to be independent of viscosity and the shape factor ( $c$ ) is constant. Machine geometry and operating conditions, such as material throughput and screw speed, determine the RVD in viscous flow regimes. To determine the role of elastic effects, the Weissenberg number ( $Wi$ ) was calculated for each polymer for conditions under which it was extruded.  $Wi$  is defined as the product of the relaxation time  $\lambda$  of the polymer and the shear rate  $\dot{\gamma}$  in the extruder. Both HDPEs had Weissenberg numbers  $< 1$ . One of the PPs had a Weissenberg number less than that for a majority of the operating conditions, whereas the one PP (PP6100) had  $Wi > 1$  for the entire range of operating conditions; it alone did not conform to the RVD model.

Based on the above analysis, it is clear that the viscoelastic nature of the polymer must be taken into account in analyzing extrusion flows. The characteristic relaxation time  $\lambda$  of the polymer has proved to be the key quantity. When  $\lambda$  is small and viscous effects dominate, the RVD model approach is valid. When  $\lambda$  is large, the elastic effects of the polymer may dominate under typical flow conditions. In this case, the model developed by Bigio et al.<sup>1</sup> probably will not apply unmodified. Further study of various polymers and operating conditions is suggested to explore the robustness of these conclusions.

## Notation

$a$  = time domain shape factor  
 $b$  = rotation domain shape factor  
 $c$  = volume domain shape factor  
 $D$  = screw diameter  
 $G'$  = storage modulus  
 $G''$  = loss modulus

$G(s)$  = residence time distribution response in the frequency domain  
 $\hat{G}(\delta)$  = residence volume distribution response in the volume frequency domain  
 $G(t)$  = residence time distribution response in the time domain  
 $h$  = screw channel depth  
 $N$  = screw speed  
 $Q$  = material throughput  
 $Q/N$  = specific throughput  
 $s$  = Laplace complex variable (frequency domain)  
 $\delta$  = Laplace complex variable (volume frequency domain)  
 $t$  = time  
 $t_d$  = time delay  
 $t_m$  = mean residence time  
 $v_d$  = volume delay  
 $v_m$  = mean residence volume

## Greek letters

$\dot{\gamma}$  = shear rate  
 $\lambda$  = characteristic relaxation time

## Abbreviations

CoTSE = corotating twin-screw extruder  
RRD = residence rotation distribution  
RTD = residence time distribution  
RVD = residence volume distribution  
 $Wi$  = Weissenberg number

## Literature Cited

1. Gao J, Walsh G, Bigio D, Briber R, Wetzel M. Residence-time distribution model for twin-screw extruders. *AIChE J.* 1999;45:2541-2549.
2. Chen T, Patterson WI, Dealy JM. On-line measurement of residence time distribution in a twin screw extruder. *Int Polym Process.* 1995; 1:3.
3. Chen L, Pan Z, Hu GH. Residence time distribution in screw extruders. *AIChE J.* 1993;39:1455.
4. Chen L, Hu GH. Applications of a statistical theory in residence time distributions. *AIChE J.* 1993;39:1558.
5. Wetzel MD, Shih CK, Sundararaj U. Comparison of RTD tracers. *SPE ANTEC Papers.* 1997;3:3707.

*Manuscript received Jun. 6, 2005, and revision received Nov. 14, 2005.*